Oscillatory Patterns in Hippocampus Under Light and Deep Isoflurane Anesthesia Closely Mirror Prominent Brain States in Awake Animals

Brian Lustig,[1,2] Yingxue Wang,[2] and Eva Pastalkova[2]*

ABSTRACT: The hippocampus exhibits a variety of distinct states of activity under different conditions. For instance the rhythmic patterns of activity orchestrated by the theta oscillation during running and REM sleep are markedly different from the large irregular activity (LIA) observed during awake resting and slow wave sleep. We found that under different levels of isoflurane anesthesia activity in the hippocampus of rats displays two distinct states, which have several qualities that mirror the theta and LIA states. These data provide further evidence that the two states are intrinsic modes of the hippocampus; while also characterizing a preparation that could be useful for studying the natural activity states in hippocampus. © 2015 Wiley Periodicals, Inc.

KEY WORDS: brain state; hippocampus; oscillations; rat; isoflurane

INTRODUCTION

Different behavioral states, such as quiet wakefulness, running, and various stages of sleep, are accompanied by different brain states. Each brain state is characterized by a unique combination of oscillations (Steriade, 1997, 2003; Buzsáki, 2002; Buzsáki and Draguhn, 2004). For example, slow-wave sleep and quiet wakefulness are both characterized by neocortical up/down states, thalamo-cortical spindles, hippocampal LIA consisting of sharp-waves (SPWs), ripples, and dentate spikes (Steriade and Deschenes, 1984; Buzsáki, 1989; Buzsáki et al., 1992; Steriade et al., 1993a,b,; Bragin et al., 1995a,b; Contreras and Steriade, 1995; Csicsvari et al., 2000; Steriade et al., 2001). In contrast, running and REM sleep (Aserinsky and Kleitman, 1953; Buzsáki, 2002) are characterized by theta and gamma oscillations in both neocortex and hippocampus (Buzsáki, 2002; Montgomery et al., 2008). Properties of individual neurons and their firing patterns also change between brain states (Steriade et al., 1993a,b, 2001; Kamondi et al., 1998; Steriade et al., 2001; Isomura et al., 2006; Marguet and Harris, 2011; Sakata and Harris, 2012; Tsuno et al., 2013). As a result, processing of the same stimulus within the same network may differ depending on the current brain state (Crochet and Petersen, 2006; Ferezou et al., 2006; Marguet and Harris, 2011). Therefore, brain states should be taken into account when studying properties of individual neurons and neuronal networks. Here we show there are two dynamic states of activity under different levels of isoflurane anesthesia and propose these states might reflect the two classical theta and LIA states typically found in behaving animals (Vanderwolf, 1969).

MATERIALS AND METHODS

All procedures were approved by the Janelia Research Campus Institutional Animal Care and Use Committee.

Animals

Ten male Long Evans rats were used for all experiments. Animals were ~400 g at the time of the study. Animals were maintained on a reversed, 12 h-long light/dark cycle.

Surgery

Eight out of ten animals were injected with AAV2/1-Syn-ReaChR-mCitrine into dorsal CA3 for reasons unrelated to this study (AP: −3.3–3.9 mm, ML: +/−3.5–4.3 mm, V: 3.3–3.4 mm). The results reported in this study did not differ between injected and noninjected animals. Three to five weeks after the viral injections, animals were anesthetized with 2% isoflurane and their heads were mounted into a stereotactic frame. In some animals, the isoflurane concentration was switched from 2 to 1% and back later during the experiment. We used a calibrated isoflurane dispenser with consistent and constant oxygen pressure to ensure reliable and reproducible delivery of specific isoflurane concentrations. Vital signs were carefully monitored throughout the surgery (MouseOx, Starr Life Sciences). An acute, 32-channel linear probe with 50 µm site spacing (Neuronexus) was lowered into hippocampus (AP: 3.2–3.5 mm, ML: 2.2–4.2 mm, V: 2.5–3.2 mm). The ground pole of the recording system was connected to muscles on the back of the animal's
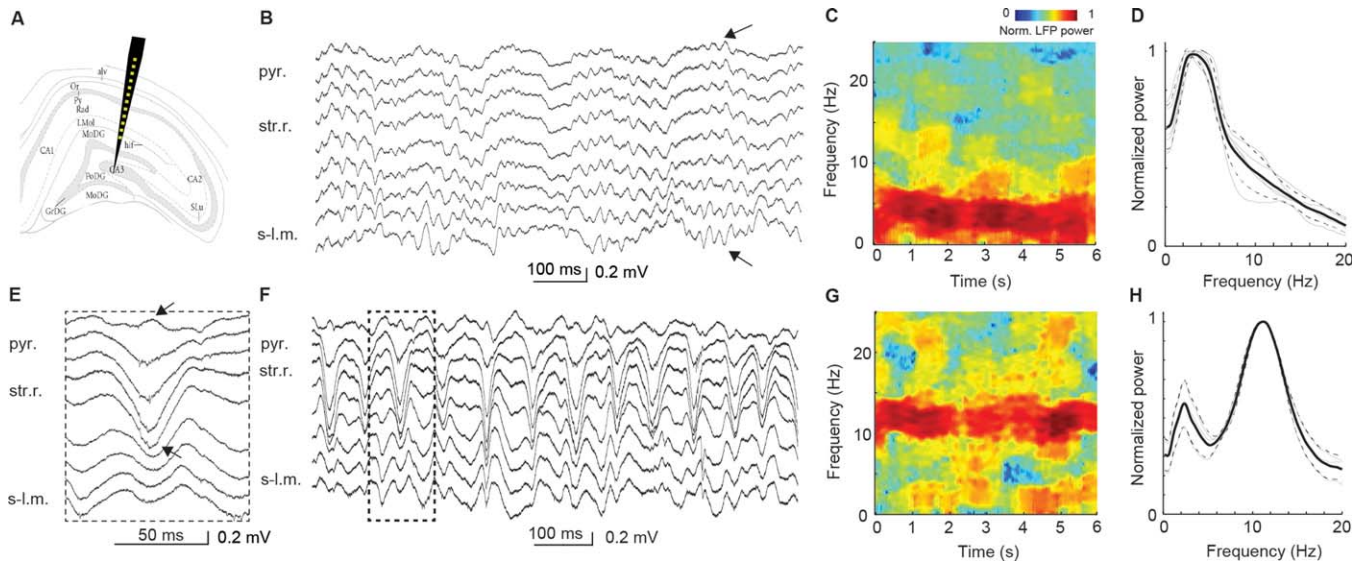
FIGURE 1.   Two distinct brain states during light and deep isoflurane anesthesia. A: Left: an approximate position of a linear probe in hippocampus. **B:** Wide band signal recorded from several hippocampal layers during light anesthesia. **C:** Spectrogram of the signal obtained from CA1 pyramidal layer during light isoflurane anesthesia. Color scale is normalized to 1. **D:** Mean power spectra of CA1 pyramidal layer signal ($N = 5$ animals) during light isoflurane anesthesia. **E:** One sharp-wave-like event recorded during deep anesthesia. Arrows point toward the maximal reversal above the pyramidal layer and in stratum radiatum. **F:** Wide band signal recorded from several hippocampal layers during deep anesthesia. One SPW-like event is marked. **G:** Spectrogram of the signal obtained from CA1 stratum radiatum layer during deep isoflurane anesthesia. **H:** Mean power spectra of stratum radiatum signal ($N = 4$ animals) during deep isoflurane anesthesia. Hippocampal layers labeling in this and the following figures: CA1 or CA3 pyramidal layer (CA1/CA3 pyr.), stratum radiatum (s.-r.), stratum lacunosum molecular (s-l.m.), and dentate gyrus granular layer (g.l.). [Color figure can be viewed in the online issue, which is available at wileyonlinelibrary.com.]

head. At the end of each experiment animals were injected with urethane (1.75 g/kg) and transcardially perfused with buffered saline and formalhyde. The position of the linear probe was confirmed histologically in each animal.

In addition two animals were chronically implanted with silicon probes (AP: −3.3, ML: −3.5, V: 3.3 mm). Brain signals were recorded first, while animals ran in a linear maze (Wang et al., 2015) and afterwards under isoflurane anesthesia in the stereotactic frame.

Electrophysiological Recordings

Data from all 32 channels were filtered (0.3 Hz–10 kHz), amplified (gain = 200) and continuously sampled at 20,833 Hz using an in-house built recording system [16 bit resolution; hardware: Whisper, software: SpikeGL (http://www.janelia.org/lab/harris-lab-apig)]. Recordings in awake animals were performed using Ampiplex (http://www.amplipex.com, Berényi et al., 2014).

Data Analysis and Statistics

Local field potential (LFP) and extracellular unit activity were analyzed in MATLAB using custom code as well as the Chronux toolbox (http://chronux.org/; Mitra and Bokil, 2008). Error bars in all figures represent standard deviation (SD). We used a nonparametric statistical test (Kolmogorov-Smirnov test) to compare experimental and shuffled-data based distributions.

Spike Sorting and Cell Classification

For spike detection, the wide-band signal was high-pass filtered (>0.8 kHz) and thresholded. Single units were first isolated semi-automatically using KlustaKwik (https://github.com/klusta-team/klustakwik, Harris et al., 2000) and refined manually using Klusters (http://neurosuite.sourceforge.net/; Hazan et al., 2006). Neurons where further classified as putative pyramidal cells, granular cells, or interneurons based on spike wave shape and firing rate (Csicsvari et al., 1999; Sirota et al., 2008). The locations of cell layers were identified by the reversal in the LFP trace polarity (Ylinen et al., 1995a; Bragin et al., 1995b; Buzsáki et al., 2003).

LFP Power

LFP spectrograms and power spectra were estimated using multitaper analysis (NW = 2, time window length 0.3–2 s length; Mitra and Pesaran, 1999).

Current Source Density

For current source density analysis the LFP traces were filtered (second-order cheby2 or butterworth filter) and interpolated before taking the second spatial derivative (Brankack et al., 1993).
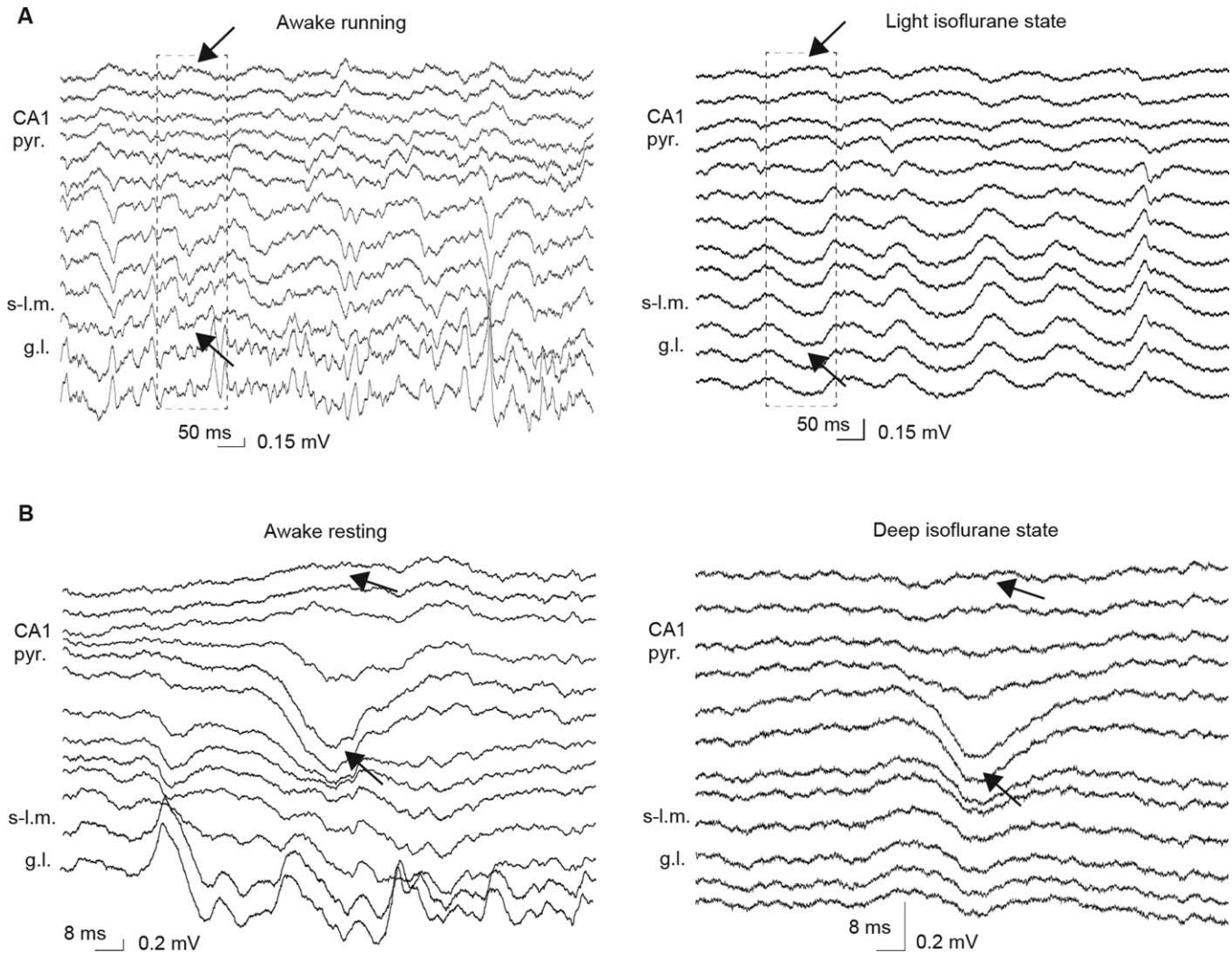
FIGURE 2.   Comparison of LFP patterns in freely behaving and anesthetized animals. A: LFP traces recorded in behaving animals during running (left) and during light anesthesia (right). B: LFP traces recorded in behaving animals during drinking (left) and during deep isoflurane anesthesia (right). Arrows point toward the maximal positive and negative reversal during each brain state.

LFP Oscillation Phase Extraction

To extract the phase of specific oscillations, the LFP was first band-pass filtered (theta: 2–5 Hz, dentate gamma: 15–25 Hz) using the second order Chebyshev type 2 filter (cheby2 MAT-LAB function). Then the instantaneous phase was estimated using the Hilbert transform.

Sharp-Wave and Dentate Spike Triggered Spike Distribution

LFP trace recorded from stratum radiatum of CA1 or from around the granular layer of dentate gyrus (DG) was band-pass filtered (the second order butterworth filter, 8–18 Hz or 10–20 Hz) and the peaks in the squared signal were detected. Spikes generated by CA1 pyramidal neurons 100 ms before and after each SPW peak were analyzed.

Transitions Between Theta and SPW States

The power in the SPW (10–15 Hz) and theta (2–4 Hz) frequency bands was estimated from signal recorded in stratum radiatum. The ratio of the mean power in the SPW and theta bands was used to determine the time point of the brain state transition as follows: theta state: ratio < 1; SPW state: ratio > 1.5.

RESULTS

We recorded neural activity and LFP using silicon probes in the hippocampus of rats anesthetized with isoflurane anesthesia. The probes were lowered into the hippocampus until their
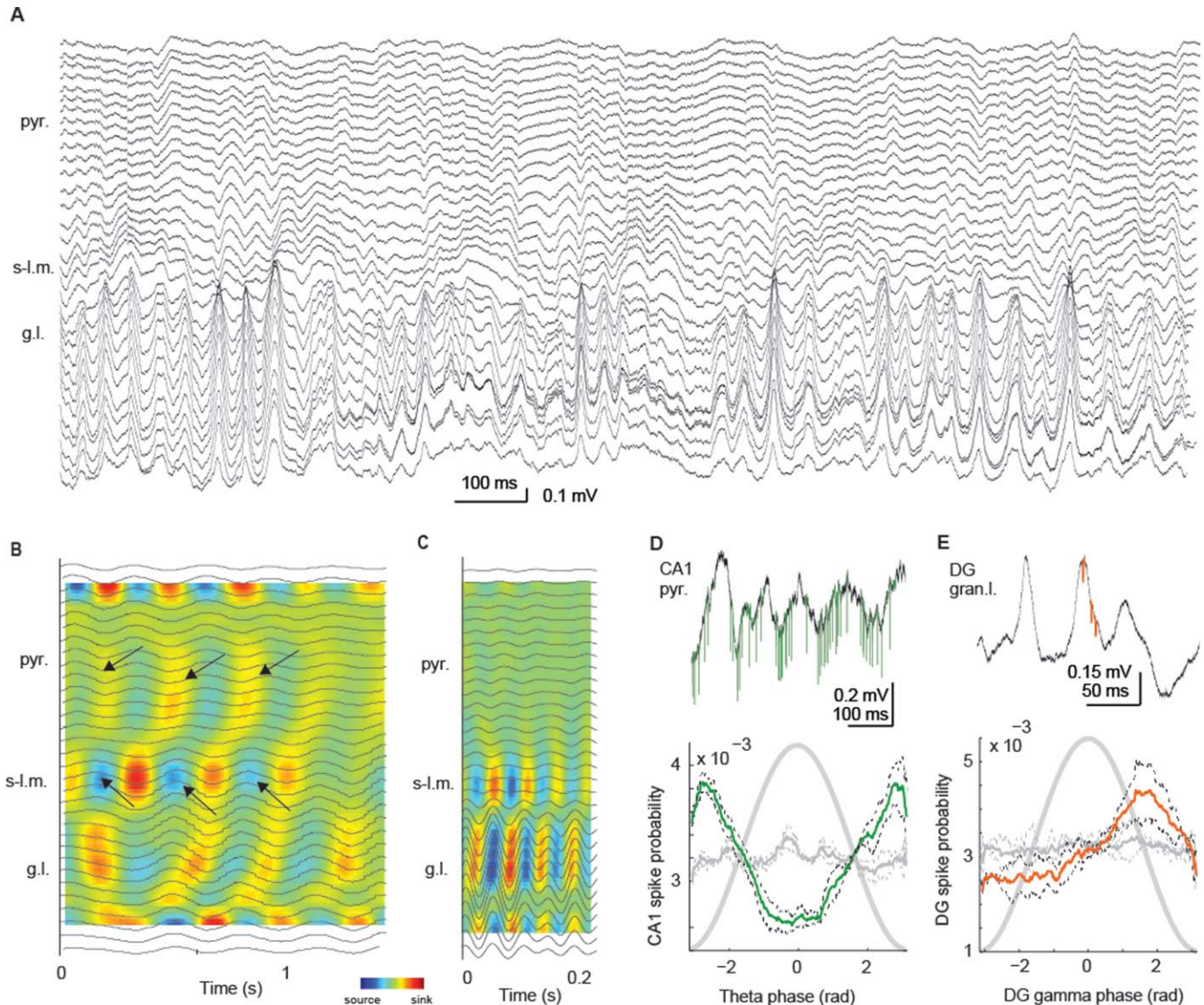
FIGURE 3.   LFP and firing patterns during light anesthesia. A: Wide band signal recorded during light anesthesia. B: Current-source density plot calculated based on signals obtained during light isoflurane anesthesia. Arrows point toward the sink-source pairs between pyr. l. and str-l. mol. C: Current-source density plot calculated based on signals recorded during light isoflurane anesthesia. D: Theta modulation of the firing of CA1 pyramidal neurons. Top: wide band trace with spikes (green). Bottom: theta phase preference of CA1 pyramidal neurons. Peak of CA1 LFP theta: 0 rad. E: Gamma modulation of dentate gyrus neurons. Top: wide band signal recorded in granular layer with spikes of putative granular cells. Bottom: gamma phase preference of putative granular neurons. Peak of DG gamma: 0 rad. [Color figure can be viewed in the online issue, which is available at wileyonlinelibrary.com.]

recording sites spanned between CA1 and CA3 pyramidal layers (Fig. 1A). While recording under different levels of isoflurane anesthesia we observed discrete oscillatory patterns (Fig. 1; Friedberg et al., 1999; Hudson et al., 2014). Recordings during the lighter level of isoflurane anesthesia (~1%) consistently displayed a slow oscillation with a peak frequency of 3.4 Hz +/–0.57 Hz (Figs. 1B–D, $n = 4$ animals). In contrast, under a deeper level of isoflurane anesthesia (~2%), hippocampal activity was dominated by an oscillation with a peak frequency of 11.18 Hz +/–0.1 Hz (Figs. 1E–H, $n = 4$ animals). Each of these oscillations lasted as long as we maintained the appropriate level of anesthesia (tens of minutes) in all tested

animals. Adjustment of the anesthesia concentration was always followed by a change of the oscillatory pattern (delay of brain state transition: from slow to fast: mean = 4.8 min, SD = 3.6 min, $n = 4$ animals; from fast to slow: mean = 10.5 min, SD = 4.2 min, $n = 3$ animals). Overall, activity in the hippocampus showed stable and unique states under light and deep isoflurane.

We asked if these two states under isoflurane anesthesia were at all related to brain states described in freely behaving animals. To answer this question we recorded hippocampal activity in two animals, first while they shuffled back and forth on a linear track for water reward (Wang et al., 2015) and then
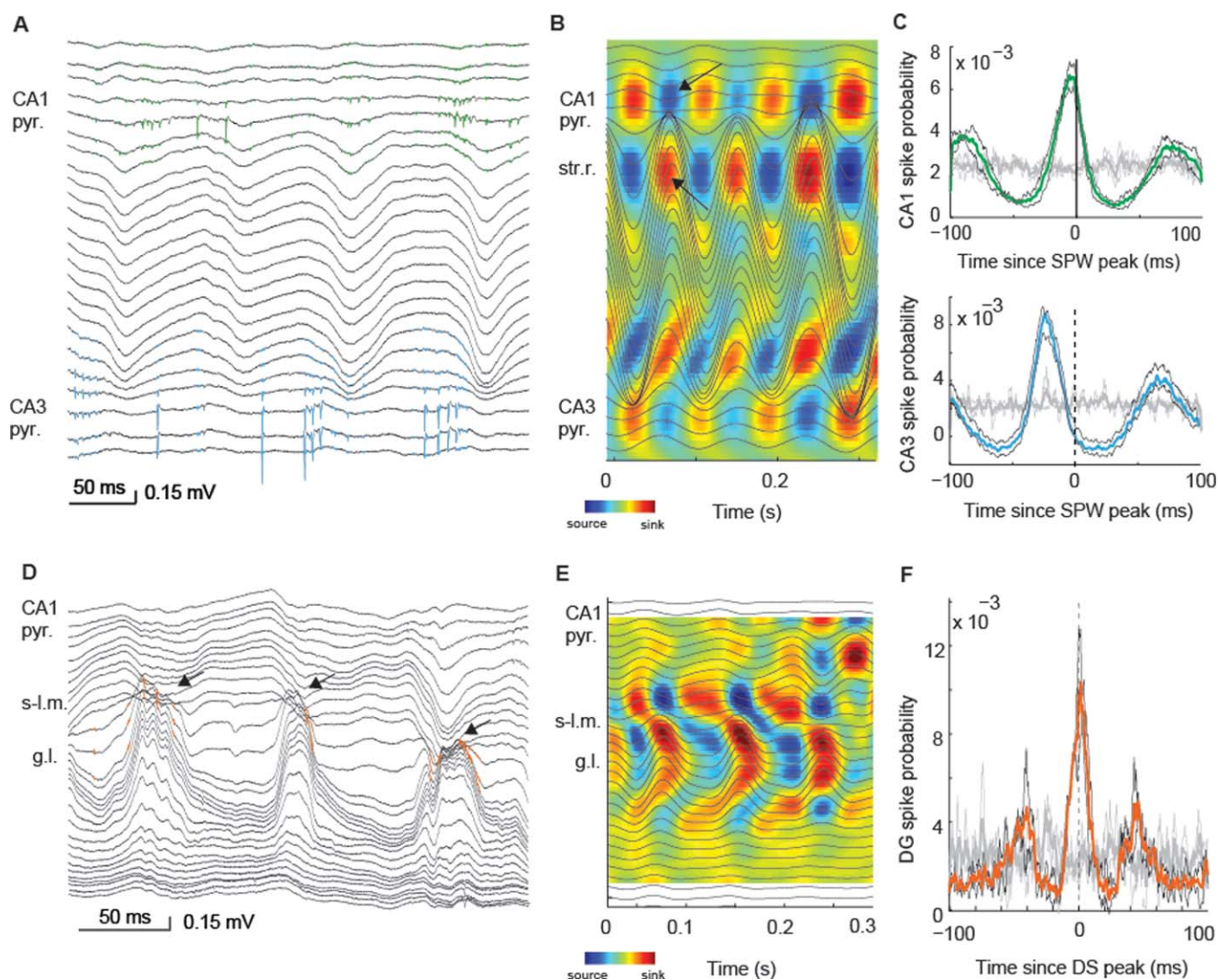
FIGURE 4. LFP and firing patterns during deep anesthesia. A: Wide band signal recorded from selected channels spanning between CA1 and CA3 pyramidal layers. Green/blue lines: action potentials generated by CA1 and CA3 neurons, respectively. B: Current-source density plot calculated based on signals recorded during deep isoflurane anesthesia. Arrows point toward sink-source pair between str. rad. and str. pyr. C: Top: Sharp-wave triggered firing probability of CA1 principal neurons. Bottom: Sharp-wave triggered firing probability of CA3 principal neurons. D: Wide band signal recorded from selected channels spanning between CA1 and DG. Arrows point toward three dentate spikes. Orange lines: action potentials generated by granular neurons. F: Current-source density plot calculated based on signals recorded during deep isoflurane anesthesia. G: Firing probability of putative granular neurons with respect to the peak of dentate spike. [Color figure can be viewed in the online issue, which is available at wileyonlinelibrary.com.]

later under isoflurane anesthesia. The depth profile of the running associated theta oscillations was strikingly similar to the slow oscillation during the light isoflurane state (∼3.5 Hz). Both showed a polarity reversal between the pyramidal and stratum lacunosum layers of CA1 (Fig. 2A). Likewise, the depth profile of SPWs during water reward and quiet resting (Buzsáki, 1986, 1989; Csicsvari et al., 2000, Buzsáki et al., 2003) was strikingly similar to the individual cycles of the ∼11 Hz oscillation during the deep isoflurane state. Both showed a polarity reversal between the pyramidal layer and stratum radiatum of CA1 (Fig. 2B). To explore whether the same mechanisms might be responsible for the generation of the brain

states in awake and isoflurane anesthetized animals we set out to characterize the properties of the isoflurane oscillations in greater detail.

First, we characterized the activity during the light isoflurane state. Current course density analysis (Brankack et al., 1993) revealed an alternating pattern of current sinks and sources localized in CA1 stratum pyramidale and stratum lacunosum moleculare (Figs. 3A,B), which strongly resembled the pattern during theta oscillations described in behaving animals (Buzsáki et al., 1983, Montgomery et al., 2008, 2009). In addition to the prominent theta-like slow oscillation during the light isoflurane state, we also observed a faster oscillation around the

granule layer of DG (18 Hz +/–3 Hz, $n = 3$ animals). The amplitude of this faster oscillation was modulated by the theta-like slow oscillation (Fig. 3A, bottom traces). CSD analysis revealed repeating current sinks and sources around the granular layer (Fig. 3C) and nicely matched the CSD pattern of typical DG-gamma oscillations previously described during running and REM sleep (Brankack et al., 1993; Bragin et al., 1995a). Importantly, activity of neurons recorded in the CA1 and DG layers was modulated by theta-like and gamma-like oscillations, respectively (Figs. 3D,E; KS-test against shuffled data, CA1: $P = 8.2e\text{-}20$, $n = 30$ pyramidal neurons from 4 animals; DG: $P = 3.6e\text{-}21$, $n = 20$ putative granular neurons from 3 animals; Buzsáki et al., 1983, Bragin et al., 1995a; Buzsáki et al., 2003) In summary, during the light isoflurane state, we observed a slow, theta-like oscillation in CA1 and a faster, gamma-like oscillation around DG. Both of these oscillations modulated the firing of local neurons.

Next, we used similar analyses to characterize the deep isoflurane state. Current source density analysis revealed an alternating pattern of sinks and sources between the CA1 pyramidal layer and stratum radiatum, which strongly resembled the CSD of repetitive SPWs (Figs. 4A,B). Individual SPW cycles lasted between 40 and 70 ms. Firing in both CA1 and CA3 neurons was strongly phase locked to the individual cycles (Fig. 4C, top). CA1 neurons tended to fire a burst of action potentials around the trough of each cycle, while the firing in CA3 neurons consistently preceded the firing of CA1 (Fig. 4C, bottom). We did not observe as prominent ripple oscillations as those reported in behaving animals (Buzsáki, 1989; Csicsvari et al., 2000). In addition to these fast oscillatory events, we frequently observed randomly interspersed sharp LFP spikes in the DG region (Fig. 4D). Current source density analysis of these fast spikes revealed sink-source pairs located around the granular layer of the dentate gyrus (Fig. 4E). Putative granular neurons fired preferentially during these spikes (Fig. 4F; KS-test against shuffled data: $P = 3.7e\text{-}27$, $n = 11$ putative granular neurons from 2 animals). These fast spikes strongly resembled previously characterized dentate spikes (Bragin et al., 1995b; Penttonen et al., 1997; Bramham, 1998; Buzsáki et al., 2003). Taken together, the patterns of activity during the deep isoflurane state was distinct from that of the light isoflurane state. Furthermore the deep isoflurane state shared several features with irregular SPW events and dentate gyrus spikes typical of LIA.

DISCUSSION

There is a large collection of literature on different brain states under anesthesia. For instance, different levels of anesthesia were associated with different neuronal responses, distinct LFP oscillations, and in some instances, novel LFP patterns (Friedberg et al., 1999; Bland et al., 2003; Hudson et al., 2014; Wolansky et al., 2006; Perouansky et al., 2010; Pignatelli et al., 2012; MacIver and Bland, 2014).

The two distinct patterns of activity we describe in this paper, recorded in hippocampus under light and deep isoflurane anesthesia (Fig. 1), have not been reported. The light isoflurane state was characterized by a prominent slow oscillation, reminiscent of theta oscillations in the awake animal. The deep isoflurane state exhibited a faster ~11 Hz oscillation that appeared distinct from anything previously reported in hippocampus, however the fundamental cycles of this oscillation had characteristics of sharp waves (Buzsáki, 1986, 1989; Csicsvari et al., 2000, Buzsáki et al., 2003). In addition, the deep isoflurane state was interspersed with LFP spikes that had characteristics of dentate spikes (Bragin et al., 1995b; Penttonen et al., 1997; Bramham, 1998; Buzsáki et al., 2003). Both, deep and light isoflurane states were maintained for extended periods of time and the switch between these states usually occurred within a few minutes after changing the concentration of isoflurane.

During the deep isoflurane state we observed rhythmically occurring SPW-like events. This was the most unexpected phenomenon we observed under isoflurane anesthesia. How could this "oscillation" be generated? In behaving animals, SPWs tend to occur in trains of two to four with an inter-SPW interval of about 100 ms (Buzsáki et al., 2003). The occurrence of SPWs is also known to be biased by thalamo-cortical spindles (10-18 Hz, Siapas and Wilson, 1998; Sirota et al., 2003) and cortical up-down states (Sullivan et al., 2011), which suggest that the hippocampal network may have a tendency to generate SPWs rhythmically. In addition, elimination of cortical and subcortical inputs into hippocampus promotes generation of more frequent and more synchronized SPWs (Buzsáki, 1986, 1989). Since isoflurane was shown to reduce cortical activity (Berg-Johnsen and Langmoen, 1990; Ferron et al., 2009; Westphalen et al., 2011; Land et al., 2012), we propose that the SPW-like oscillation during the deep isoflurane state might reflect a native tendency within the hippocampal network to generate SPWs rhythmically.

During the light isoflurane state, a prominent theta-like oscillation was continuously present. This was also a rather unexpected observation because typically under urethane anesthesia theta oscillation in hippocampus is only induced for brief periods of time by tail pinch or pedunculopontine tegmental nucleus stimulation (Kramis et al., 1975; Sakata and Harris, 2012). Furthermore, when not under anesthesia short bouts of theta (a few seconds to a few minutes) are frequently observed in running animals and during REM sleep. Thus, activity in the hippocampus under light and deep isoflurane anesthesia might be reflective of a natural tendency of the hippocampal circuit to produce either theta-like or sharp-wave-like oscillations.

Different brain states are accompanied by largely differing single cell properties, single-cell firing patterns, levels of neuromodulation, and neuronal interactions. However, studying how these parameters change with brain state is frequently very difficult or impossible in freely moving or head-fixed animals. Therefore, testing hypotheses in anesthetized animals might be the only available or vastly more efficient option in many studies.

Overall, we have shown that light and deep isofurane anesthesia was accompanied by continuous theta-like and SPW-like states respectively, and thus provide evidence that these two states represent default states of the hippocampal circuit. This finding can be used when studying brain-state-dependent cell and network properties and interactions.

Acknowledgments

REFERENCES

Aserinsky E, Kleitman N. 1953. Regularly occurring periods of eye motility, and concomitant phenomena, during sleep. Science 118: 273–274.

Berényi A, Somogyvári Z, Nagy AJ, Roux L, Long JD, Fujisawa S, Stark E, Leonardo A, Harris TD, Buzsáki G. 2014. Large-scale, high-density (up to 512 channels) recording of local circuits in behaving animals. J Neurophysiol 111:1132–1149.

Berg-Johnsen J, Langmoen IA. 1990. Mechanisms concerned in the direct effect of isoflurane on rat hippocampal and human neocortical neurons. Brain Res 507:28–34.

Bland BH, Bland CE, Colom LV, Roth SH, DeClerk S, Dypvik A, Bird J, Deliyannides A. 2003. Effect of halothane on type 2 immobility related hippocampal theta field activity and theta-on/theta-off cell dischanrges. Hippocampus 13:38–47.

Bragin A, Jandó G, Nádasdy Z, Hetke J, Wise K, Buzsáki G. 1995a. Gamma (40-100 Hz) oscillation in the hippocampus of the behaving rat. J Neurosci 15:47–60.

Bragin A, Jandó G, Nádasdy Z, van Landeghem M, Buzsáki G. 1995b. Dentate EEG spikes and associated interneuronal population bursts in the hippocampal hilar region of the rat. J Neurophysiol 73:1691–1705.

Bramham CR. 1998. Phasic boosting of medial perforant path-evoked granule cell output time-locked to spontaneous dentate EEG spikes in awake rats. J Neurophysiol 79:2825–2832.

Brankack J, Stewart M, Fox SE. 1993. Current source density analysis of the hippocampal theta rhythm: Associated sustained potentials and candidate synaptic generators. Brain Res 615:310–327.

Buzsáki G. 1986. Hippocampal sharp waves: Their origin and significance. Brain Res 398:242–252.

Buzsáki G. 1989. Two-stage model of memory trace formation: A role for "noisy" brain states. Neuroscience 31:551–570.

Buzsáki G. 2002. Theta oscillations in the hippocampus. Neuron 33: 325–340.

Buzsáki G, Draguhn A. 2004. Neuronal oscillations in cortical networks. Science 304:1926–1929.

Buzsáki G, Leung LW, Vanderwolf CH. 1983. Cellular bases of hippocampal EEG in the behaving rat. Brain Res 287:139–171.

Buzsáki G, Horváth Z, Urioste R, Hetke J, Wise K. 1992. High-frequency network oscillation in the hippocampus. Science 256: 1025–1027.

Buzsáki G, Buhl DL, Harris KD, Csicsvari J, Czéh B, Morozov A. 2003. Hippocampal network patterns of activity in the mouse. Neuroscience 116:201–211.

Contreras D, Steriade M. 1995. Cellular basis of EEG slow rhythms: A study of dynamic corticothalamic relationships. J Neurosci 15: 604–622.

Crochet S, Petersen CC. 2006. Correlating whisker behavior with membrane potential in barrel cortex of awake mice. Nat Neurosci 9:608–610.

Csicsvari J, Hirase H, Czurkó A, Mamiya A, Buzsáki G. 1999. Oscillatory coupling of hippocampal pyramidal cells and interneurons in the behaving Rat. J Neurosci 19:274–287.

Csicsvari J, Hirase H, Mamiya A, Buzsáki G. 2000. Ensemble patterns of hippocampal CA3-CA1 neurons during sharp wave-associated population events. Neuron 28:585–594.

Ferezou I, Bolea S, Petersen CC. 2006. Visualizing the cortical representation of whisker touch: Voltage-sensitive dye imaging in freely moving mice. Neuron 50:617–629.

Ferron JF, Kroeger D, Chever O, Amzica F. 2009. Cortical inhibition during burst suppression induced with isoflurane anesthesia. J Neurosci. 29:9850–9860.

Friedberg MH, Lee SM, Ebner FF (1999) Modulation of receptive field properties of thalamic somatosensory neurons by the depth of anesthesia. J Neurophysiol 81:2243–2252.

Isomura Y, Sirota A, Ozen S, Montgomery S, Mizuseki K, Henze DA, Buzsáki G. 2006. Integration and segregation of activity in entorhinal-hippocampal subregions by neocortical slow oscillations. Neuron 52:871–882.

Harris KD, Henze DA, Csicsvari J, Hirase H, Buzsáki G. 2000. Accuracy of tetrode spike separation as determined by simultaneous intracellular and extracellular measurements. J Neurophysiol 84: 401–414.

Hazan L, Zugaro M, Buzsáki G. 2006. Klusters, NeuroScope, NDManager: A free software suite for neurophysiological data processing and visualization. J Neurosci Methods 155:207–216.

Hudson AE, Calderon DP, Pfaff DW, Proekt A. 2014. Recovery of consciousness is mediated by a network of discrete metastable activity states. Proc Natl Acad Sci U S A 111:9283–9288.

Kamondi A, Acsády L, Wang XJ, Buzsáki G. 1998. Theta oscillations in somata and dendrites of hippocampal pyramidal cells in vivo: Activity-dependent phase-precession of action potentials. Hippocampus 8:244–261.

Kramis R, Vanderwolf CH, Bland BH. 1975. Two types of hippocampal rhythmical slow activity in both the rabbit and the rat: Relations to behavior and effects of atropine, diethyl ether, urethane, and pentobarbital. Exp Neurol 49:58–85.

Land R, Engler G, Kral A, Engel AK. 2012. Auditory evoked bursts in mouse visual cortex during isoflurane anesthesia. PLoS One 7: e49855-

MacIver MB, Bland BH. 2014. Chaos analysis of EEG during isoflurane-induced loss of righting in rats. Front Syst Neurosci 16:203.

Marguet SL, Harris KD. 2011. State-dependent representation of amplitude-modulated noise stimuli in rat auditory cortex. J Neurosci 31:6414–6420.

Mitra PP, Bokil H (2008) Observed brain dynamics. Oxford University Press, New York, USA.

Mitra PP, Pesaran B. 1999. Analysis of dynamic brain imaging data. Biophys J 76:691–708.

Montgomery SM, Sirota A, Buzsáki G. 2008. Theta and gamma coordination of hippocampal networks during waking and rapid eye movement sleep. J Neurosci 28:6731–6741.

Montgomery SM, Betancur MI, Buzsáki G. 2009. Behavior-dependent coordination of multiple theta dipoles in the hippocampus. J Neurosci 29:1381–1394.

Penttonen M, Kamondi A, Sik A, Acsády L, Buzsáki G. 1997. Feed-forward and feed-back activation of the dentate gyrus in vivo during dentate spikes and sharp wave bursts. Hippocampus 7:437–450.

Perouansky M, Rau V, Ford T, Oh SI, Perkins M, Eger EI2, Pearce RA. 2010. Slowing of the hippocampal θ rhythm correlates with anesthetic-induced amnesia. Anesthesiology 113:1299–1309.

Pignatelli M, Beyeler A, Leinekugel X. 2012. Neural circuits underlying the generation of theta oscillations. J Physiol Paris 106:81–92.

Sakata S, Harris KD. 2012. Laminar-dependent effects of cortical state on auditory cortical spontaneous activity. Front Neural Circuits 6:109.

Siapas AG, Wilson MA. 1998. Coordinat ed interactions between hippocampal ripples and cortical spindles during slow-wave sleep. Neuron 21:1123–1128.

Sirota A, Csicsvari J, Buhl D, Buzsáki G. 2003. Communication between neocortex and hippocampus during sleep in rodents. Proc Natl Acad Sci U S A 100:2065–2069.

Sirota A, Montgomery S, Fujisawa S, Isomura Y, Zugaro M, Buzsáki G. 2008. Entrainment of neocortical neurons and gamma oscillations by the hippocampal theta rhythm. Neuron 60:683–697.

Steriade M. 1997. Synchronized activities of coupled oscillators in the cerebral cortex and thalamus at different levels of vigilance. Cereb Cortex 7:583–604.

Steriade M. 2003. The corticothalamic system in sleep. Front Biosci 8:d878–899.

Steriade M, Deschenes M. 1984. The thalamus as a neuronal oscillator. Brain Res 320:1–63.

Steriade M, McCormick DA, Sejnowski TJ. 1993a. Thalamocortical oscillations in the sleeping and aroused brain. Science 262:679–685.

Steriade M, Nuñez A, Amzica F. 1993b. A novel slow (< 1 Hz) oscillation of neocortical neurons in vivo: depolarizing and hyperpolarizing components. J Neurosci 13:3252–3265.

Steriade M, Timofeev I, Grenier F. 2001. Natural waking and sleep states: A view from inside neocortical neurons. J Neurophysiol 85:1969–1985.

Sullivan D, Csicsvari J, Mizuseki K, Montgomery S, Diba K, Buzsáki G. 2011. Relationships between hippocampal sharp waves, ripples, and fast gamma oscillation: Influence of dentate and entorhinal cortical activity. J Neurosci 31:8605–8616.

Tsuno Y, Schultheiss NW, Hasselmo ME. 2013. In vivo cholinergic modulation of the cellular properties of medial entorhinal cortex neurons. J Physiol 591:2611–2627.

Westphalen RI, Kwak NB, Daniels K, Hemmings HCJ. 2011. Regional differences in the effects of isoflurane on neurotransmitter release. Neuropharmacology 61:699–706.

Vanderwolf CH. 1969. Hippocampal electrical activity and voluntary movement in the rat. Electroencephalogr. Clin Neurophysiol 26:407–418.

Wang Y, Romani S, Lustig B, Leonardo A, Pastalkova E. 2015. Theta sequences are essential for internally generated hippocampal firing fields. Nat Neurosci 18:282–288.

Wolansky T, Clement EA, Peters SR, Palczak MA, Dickson CT. 2006. Hippocampal slow oscillation: A novel EEG state and its coordination with ongoing neocortical activity. J Neurosci 26:6213–6229.

Ylinen A, Bragin A, Nádasdy Z, Jandó G, Szabó I, Sik A, Buzsáki G. 1995a. Sharp wave-associated high-frequency oscillation (200 Hz) in the intact hippocampus: Network and intracellular mechanisms. J Neurosci 15:30–46.